

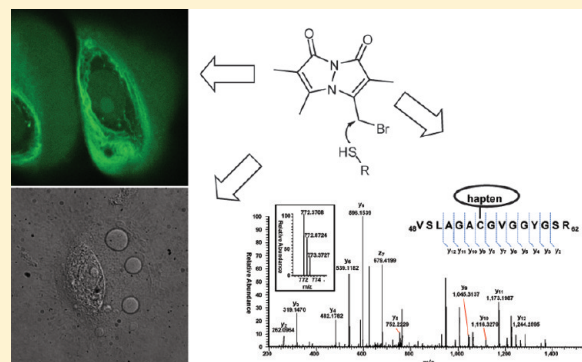
Modification and Expulsion of Keratins by Human Epidermal Keratinocytes upon Hapten Exposure in Vitro

Brigitte Bauer,^{*,†} Sofia I. Andersson,[‡] Anna-Lena Stenfeldt,[‡] Carl Simonsson,[‡] Jörgen Bergström,[§] Marica B. Ericson,[†] Charlotte A. Jonsson,[‡] and Kerstin S. Broo[‡]

[†]Department of Physics, [‡]Department of Chemistry, Dermatochemistry and Skin Allergy, and [§]Proteomics Core Facility, University of Gothenburg, 412 96 Gothenburg, Sweden

S Supporting Information

ABSTRACT: Allergic contact dermatitis is the most prevalent form of human immunotoxicity. It is caused by reactive low molecular weight chemicals, that is, haptens, coming in contact with the skin where hapten–peptide complexes are formed, activating the immune system. By using sensitizing fluorescent thiol-reactive haptens, that is, bromobimanes, we show how keratinocytes respond to hapten exposure in vitro and reveal, for the first time in a living system, an exact site of haptentation. Rapid internalization and reaction of haptens with keratin filaments were visualized. Subsequently, keratinocytes respond in vitro to hapten exposure by release of membrane blebs, which contain haptentated keratins 5 and 14. Particularly, cysteine 54 of K5 was found to be a specific target. A mechanism is proposed where neoepitopes, otherwise hidden from the immune system, are released after hapten exposure via keratinocyte blebbing. The observed expulsion of modified keratins by keratinocytes in vitro might play a role during hapten sensitization in vivo and should be subject to further investigations.



INTRODUCTION

Allergic contact dermatitis (ACD) is considered to be the most widespread form of immunotoxicity, which is instigated when reactive molecules of low molecular weight, that is, haptens, come into contact with skin.¹ More than 4000 substances are found to cause ACD,² and the prevalence of ACD in the adult population in Europe is 15–20%.³ ACD cannot be cured; thus, a sensitized individual has to avoid the chemical that elicits the allergic reaction. This can be challenging when several haptens are present as preservatives or fragrant terpenes in everyday products, for examples, detergents, soaps, and cosmetic products. Research for fundamental understanding of the processes involved in ACD is crucial not only for improved diagnostics and treatment of ACD but also to develop reliable in vitro tests for identification of potential haptens. The skin's role as the main barrier protecting the body, for example, from dehydration, mechanical injury, and the entry of microorganisms, is illustrated by the physicochemical properties of the stratified layer, but unfortunately, this layer allows the penetration of ACD-inducing haptens. Generally, haptens are too small to activate the adaptive immune response. Instead, the formation of immunogenic hapten–protein complexes (HPC) by covalent linkage of the reactive hapten to a carrier protein is recognized as one of the key events for triggering the immune system.⁴ These immunogenic complexes are consequently processed and presented

by dendritic cells (DC) of the skin to naïve T lymphocytes in the lymph nodes, thereby activating the adaptive immune system.

Although this mechanism is generally accepted, no in vivo protein targets were identified, until recently. Interestingly, our latest study⁵ revealed that in the basal layer, specific keratin intermediate filament (KIF) proteins are targeted when exposing skin tissue to bromobimanes, which are thiol-reactive fluorescent model haptens. The bromobimanes are strong contact sensitizers according to the local lymph node assay (LLNA),⁵ the preferred method today to detect and classify contact allergens.⁶ To the best of our knowledge, this is the first time that specific haptent-labeled proteins, including an explicitly targeted amino acid, have been identified in human skin. It is important to note that other hapten–protein targets have been studied as well,^{7–12} although these were model proteins and in contrast to our studies, not proven to be hapten targets also in vivo.

Given the fact that keratinocytes constitute the main component of the epidermis, keratinocyte-derived proteins would be likely hapten targets. However, most studies regarding the active role of keratinocytes in the mechanism of ACD have been focused on cytokine and chemokine secretion after hapten exposure, leading to, for example, DC migration or attracting leukocytes.^{13,14} Some reports show that keratinocytes might also act as antigen

Received: January 19, 2011

Published: April 12, 2011

presenting cells, leading to T-cell unresponsiveness,¹⁵ but investigations focusing on keratinocyte-derived proteins as hapten targets are largely missing.

As the recent insights on hapten binding and localization were gained in excised skin tissue, we, as the next step, sought to employ keratinocytes *in vitro* to confirm the hapten target sites, reveal their exact molecular location, and investigate the cellular response upon hapten exposure. For this, we exposed cultured primary human keratinocytes to the same model haptens used in the previous study—the bromobimanes. These probes have proven to be suitable for this purpose as they are strong sensitizers and become fluorescent upon binding to thiol groups.⁵ First, we used epifluorescence and confocal microscopy to visualize cellular localization of HPC. An intriguing cellular response of keratinocytes to hapten exposure was the shedding of micrometer-sized fluorescent cell membrane blebs. Following this observation, mass spectrometry techniques were employed to analyze the bleb content, with the hypothesis that HPCs are enclosed. Furthermore, *in vivo* studies have indicated the production of keratin 14 (K14) antibodies upon hapten exposure.⁵ We thus propose a hypothesis where haptens are taken up by keratinocytes, bind to keratins, and subsequently are expelled as HPCs, which can then be recognized by the immune system as neopeptides.

EXPERIMENTAL PROCEDURES

Cell Culture. Normal human epidermal keratinocytes (HEKn, Cascade Biologics, Portland, OR) were maintained in phenol red-free EpiLife keratinocyte medium (Cascade Biologics) supplemented with 60 μ M CaCl₂, gentamicin/amphotericin, and 1% (v/v) human keratinocyte growth supplement (HKGS; Cascade Biologics) at 37 °C in a humidified 5% CO₂ incubator. The final concentrations of the components in the supplemented medium were as follows: bovine pituitary extract, 0.2% v/v; bovine insulin, 5 mg/mL; hydrocortisone, 0.18 mg/mL; bovine transferrin, 5 mg/mL; human epidermal growth factor, 0.2 ng/mL; gentamicin, 10 μ g/mL; and amphotericin B, 0.25 μ g/mL. The keratinocytes were used for experiments in the fifth or sixth passage.

Cells were seeded on Ø 35 mm glass bottom dishes (P35G-1.5-14-C; MatTek, Ashland, MA) at an initial density of $\sim 1 \times 10^3$ cells/cm². Experiments on cells were performed after 2–3 days of cell growth.

Live Cell Imaging. Stock solutions of bimanes [50 mM; monobromobimane (mBBR), dibromobimane (dBBR), and methylbimane, Sigma Aldrich] were prepared in acetonitrile or DMSO (Sigma Aldrich). Stock solutions in DMSO were freshly prepared prior to experiments. The cell medium was removed and washed twice with HEPES imaging buffer (140 mM NaCl, 20 mM HEPES, 5 mM KCl, 1 mM MgCl₂, 0.06 mM CaCl₂, and 10 mM D-glucose). For incubation with bimanes, HEPES imaging buffer was supplemented with 0.05 mM mBBR, 0.5 mM dBBR, and 0.5 mM methylbimane, respectively. Bimane solution, 1 mL, was added to the cell layer and incubated for 10–15 min. To reduce background fluorescence, incubation solution was removed, and the cell layer was washed twice and immersed in 1 mL of HEPES imaging buffer.

Epifluorescence imaging was performed using a Nikon TE300 inverted microscope. Bimanes were excited using a mercury-arc lamp with fluorescence emission passing through a FF01 479/40 emission filter, and images were taken using a Kappa CCD camera (Gleichen, Germany). Confocal images were obtained using a Leica TCS SP2 RS (Wetzlar, Germany) with a PL APO CS 63 \times /1.2W CORR objective. The 350 nm UV laser line was used for excitation, and emission was collected using a photomultiplier tube with a sensitivity set in the 450–600 nm spectra. For the time lapse studies, images were taken immediately after exchange of bimane solution with HEPES imaging buffer. Cells were typically observed up to ~ 4 h.

Local Perfusion of Cells. Borosilicate micropipets with an orifice of 500 nm were pulled on a CO₂ laser puller instrument (model P-2000; Sutter Instrument). A microinjection system (CellTram vario; Eppendorf) was used to control perfusion. High-graduation micromanipulators (MWH-3; Narishige) allowed precise control of pipet positioning. For perfusion, a cell or cell cluster was selected, the pipet was filled with 0.05 mM mBBR and positioned close to the cell, and a continuous flow was applied. Time-lapse imaging was started directly after flow initiation (lag time ~ 10 s), and images were taken at an interval of 6 s for a total time of up to ~ 8 min.

Apoptosis Test. Before treatment, the respective cell dishes were washed with PBS and incubated with 0.25 mM mBBR, HEPES buffer as a negative control, or 0.5 mM H₂O₂ as a positive control. Cells were stained 4 and 7.5 h postincubation with Alexa-Fluor 488-conjugated annexin V and PI using the Vybrant apoptosis assay kit from Molecular Probes (Eugene, OR) following the manufacturer's protocol.

Extraction of Cell Blebs. Keratinocytes were grown in 75 cm² flasks at an initial density of $\sim 1.8 \times 10^5$ cells/cm² and cultured until 70–80% confluence. A 50 mM stock solution of mBBR was diluted to 0.05 mM in 5 mL of HEPES imaging buffer (140 mM NaCl, 20 mM HEPES, 5 mM KCl, 1 mM MgCl₂, 0.06 mM CaCl₂, and 10 mM D-glucose). The cell layer was washed with HEPES imaging buffer and incubated with the mBBR containing solution for 24 h at 37 °C in a 5% CO₂ humidified incubator. The cell blebs were isolated from the supernatant obtained by centrifugation of cell medium-containing cells and blebs at 500g for 5 min at room temperature.

SDS-PAGE and Western Blot. The blebs in the supernatant were lysed with 4 \times freeze–thaw cycles using ethanol, dry ice, and a 37 °C water bath. The lysate was concentrated and desalted in 5 kDa MWCO 4 mL Agilent Spin Concentrators for Proteins (Agilent Technologies). The total protein concentration was determined with BCA Protein Assay (Pierce). The concentrate was stored at -20 °C until use.

The samples were diluted [46 μ g, 30 μ L; K14 and keratin 5 (K5): 0.2 μ g, 5 μ L] with XT Sample Buffer 4X (BioRad), SDS buffer (100 mM SDS and 100 mM Tris), and Milli-Q grade water (Millipore). Electrophoresis was performed (200 V, 400 mA, 50 W, 50 min) using MOPS running buffer. Gels were fixed and coomassie-stained (Bio-Safe Coomassie G-250, BioRad). Unfixed gels were blotted (70 V, 400 mA, 50 W, 30 min) onto polyvinylidene difluoride membranes (BioRad). The blots were blocked for 2 h in buffer containing 50 mM Tris-HCl, 0.2 M NaCl, and 3% nonfat dry milk (BioRad), incubated for 1 h with primary K5 or K14 guinea pig anti-human polyclonal antibodies (Lifespan Biosciences; 1:5000) and incubated for 30 min with peroxidase-rabbit anti-guinea pig IgG (H+L) secondary antibody (Invitrogen; 1:2000). The blots were washed 3 \times 10 min with buffer consisting of 50 mM Tris-HCl, 0.2 M NaCl, and 0.05% Tween-20 (Sigma-Aldrich) between each step and developed with DAB (3,3'-Diaminobenzidine).

Nano-LC-MS/MS. Excised protein bands from the coomassie-stained gel were analyzed using nano-LC-MS/MS. See the Supporting Information for detailed experimental protocols.

Two-Photon Fluorescence Imaging of Skin Tissue. Full thickness human skin obtained from breast reduction surgery was exposed to bimane solutions for 20 h and imaged using a two-photon fluorescence microscope, as earlier described by Simonsson et al.³ For a detailed description of the experimental procedure, see the Supporting Information.

RESULTS

Bimane Internalization and Localization in Living Keratinocytes. The formation of HPC by the bromobimanes was tracked on the cellular level by exposing cultured, undifferentiated primary human keratinocytes to the model haptens mBBR and dBBR and visualized using epifluorescence and confocal microscopy (Figure 1). The permanently fluorescent methylbimane served as a

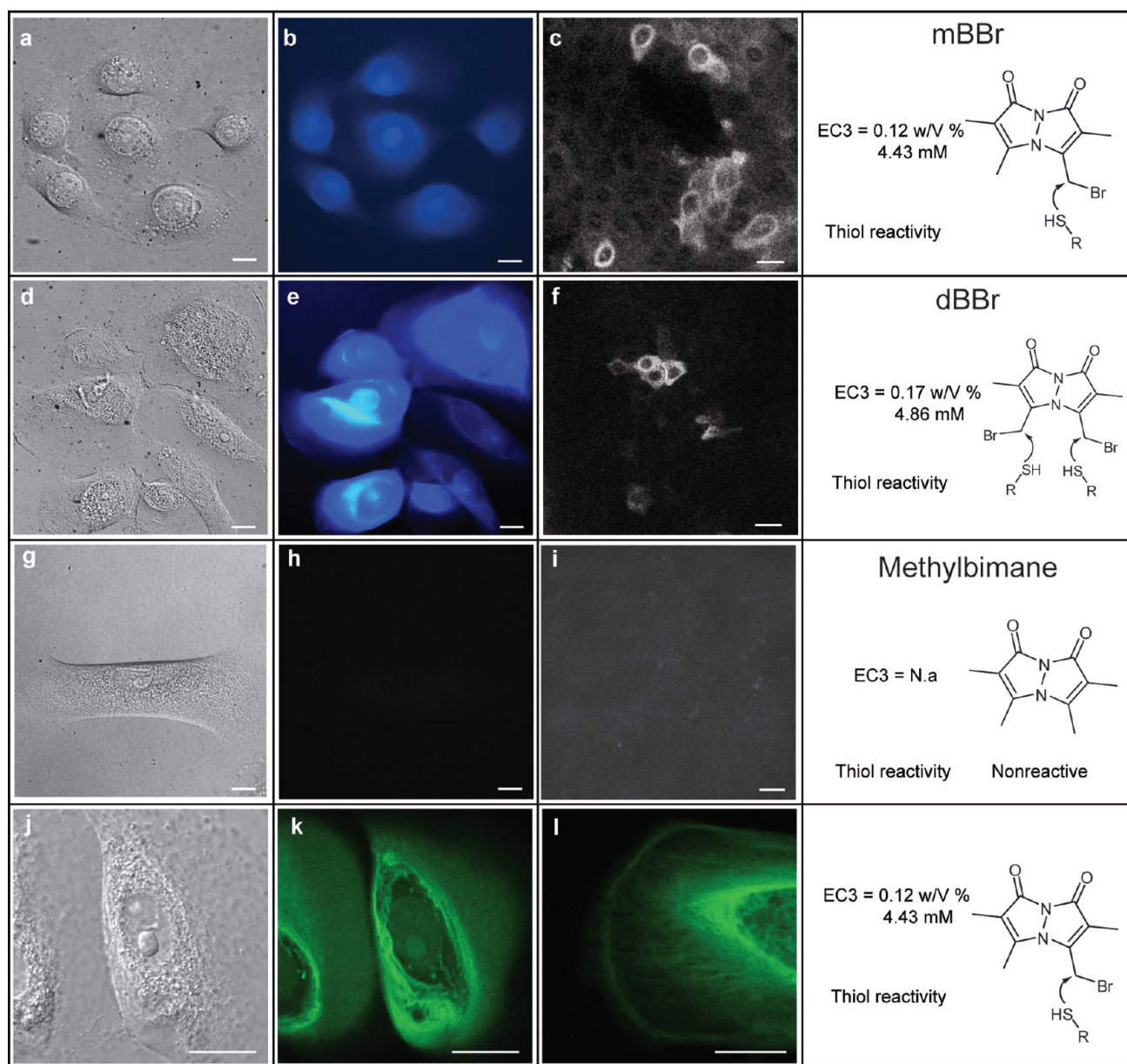


Figure 1. Microscopy images of bimane uptake in cultured keratinocytes and skin tissue. (a, d, and g) DIC images of keratinocytes after hapten exposure. (b, e, and h) Epifluorescence images showing (b) mBBr and (e) dBBr fluorescence 15 min after exposure and (h) methylbimane fluorescence 1 h after exposure. (c, f, and i) Two-photon fluorescence images of the basal keratinocyte layer in excised skin tissue exposed to (c) mBBr, (f) dBBr, and (i) methylbimane. Images were adapted from ref 5. (j) Transmitted light image corresponding to (k), a confocal image of mBBr binding in keratinocytes as is (l). The right panel shows sensitization potential (EC3 values derived from the LLNA) and reactivity characteristics of the different bimanes.⁵ Scale bars correspond to 20 μ m.

nonreactive control. Cultured keratinocytes (Figure 1a,d,g,j) displayed a similar intracellular localization of the bimanes mBBr and dBBr (Figure 1b,e). Internalization takes place within seconds, demonstrated by locally perfusing a single keratinocyte with mBBr while detecting intracellular fluorescence build-up over time (Supporting Information, video 1). Confocal microscopy images of mBBr exposed keratinocytes revealed a strong filamentous character of HPCs, stretching out through the cell and toward the cell periphery (Figure 1k,l). This filamentous pattern could also be rapidly detected within a minute after local perfusion of a cell cluster (Supporting Information, video 2). In both time-lapse studies, intracellular fluorescence was detected already in the first

image frame obtained after an instrumental lag time of ~ 10 s, demonstrating the rapid uptake of mBBr. The uniform fluorescence visible in the cytosol, nucleus, and nucleolus can most likely be ascribed to the abundant glutathione transferases (GSH) that are known to catalyze the conjugation of intracellular GSH with bromobimanes.¹⁶ Keratinocytes exposed to the permanently fluorescent nonreactive analogue methylbimane did not show any localized uptake (Figure 1h). To detect any uptake at all, high concentrations were required, and nonspecific intracellular distribution was found. The uptake pattern in excised skin tissue (Figure 1c, f), incubated for 20 h, is comparable to the observed uptake in cell cultures. In the two-photon microscopy images of bimane-exposed

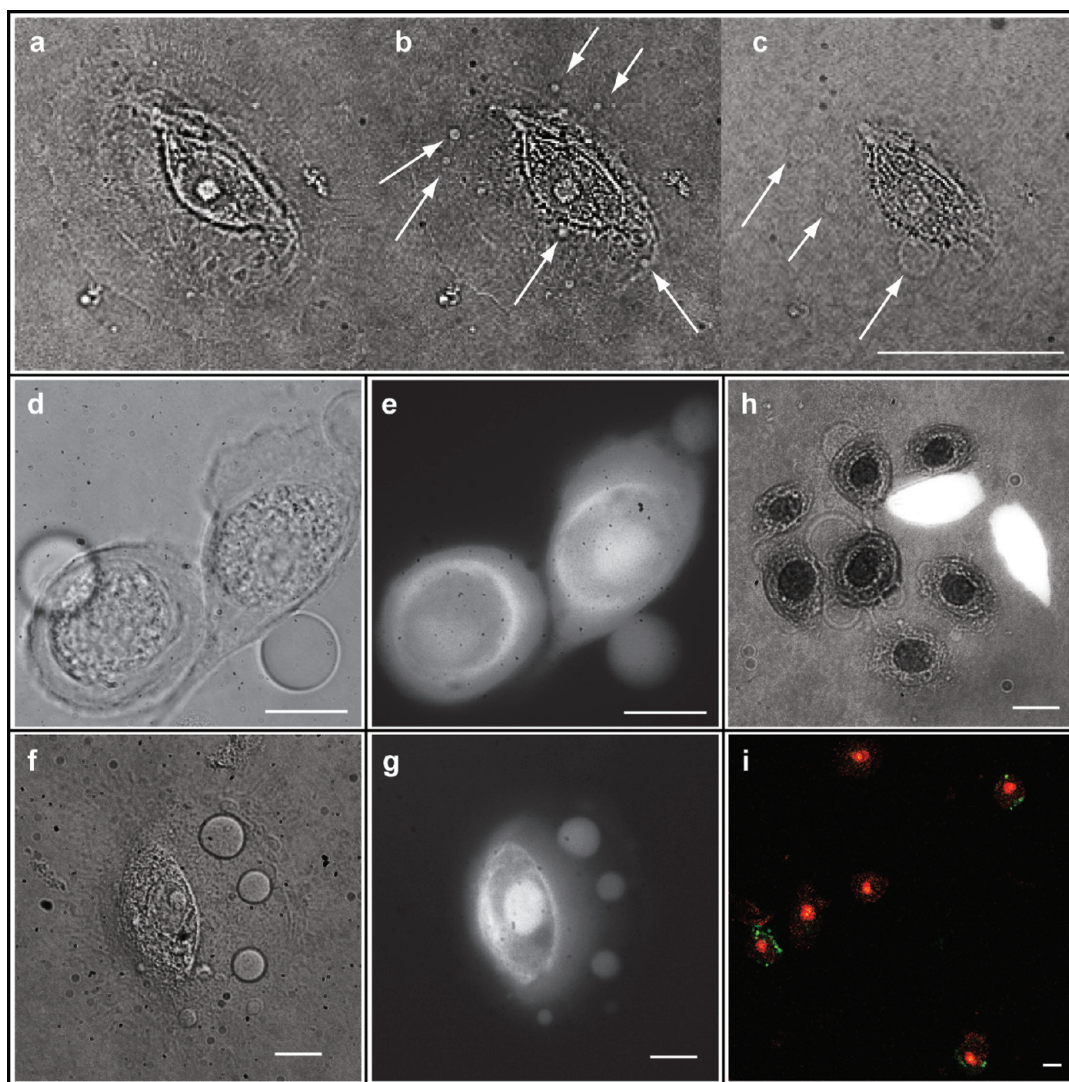


Figure 2. Microscopy images showing blebbing response and apoptosis staining of keratinocytes after bimane exposure. (a–c) DIC images showing bleb development and growth over time (~ 2 h) after 10–15 min of exposure to mBBr. (d and e) DIC and epifluorescence image of blebs on keratinocytes 2 h after mBBr exposure. (f and g) DIC and epifluorescence image of blebs on keratinocytes 1 h after dBBr exposure. (h) Overlay DIC/epifluorescence image of keratinocytes after ~ 4 h of mBBr exposure subjected to trypan blue staining. Cells that have taken up trypan blue (dark cells) have lost intracellular fluorescence and are releasing blebs. In the same colony, viable cells still exhibit bimane fluorescence (white due to overexposure). (i) Confocal images of cells probed for PS externalization (green) and PI (red) uptake after mBBr exposure for 7 h. Only cells with compromised membranes (necrotic cells) could be detected. Most cells displayed strong nuclear staining, and on a few cells, detectable PS labeling via binding to the inner leaflet of the plasma membrane could be observed. Scale bars correspond to $20\ \mu\text{m}$.

skin tissue, distinct fluorescence in the cytosolic region of the basal epidermal layer could be visualized (Supporting Information). The reason why fractions of cell clusters in this layer were the main hapten targets is unclear, but in further investigations, the targeted cells were identified as keratinocytes. In addition, the distribution pattern of the labeled cells (Figure 1c,f) has indicated that they might in fact be keratinocyte stem cells.⁵ Furthermore, keratinocytes in the suprabasal layers were weakly stained, possibly due to low availability of free thiols. Like in keratinocyte cultures, no significant uptake of methylbimane was detected in human skin (Figure 1i).

Keratinocytes Release Membrane Blebs upon Hapten Exposure. To explore the long-term biological response of cells upon haptenation, keratinocytes were exposed to the bimanes and imaged for up to 24 h postexposure. Unexpectedly, 1–2 h after hapten exposure, micrometer-sized fluorescent membrane blebs

started to form at the cell surface (Figure 2a–c). Within 10–15 min after initiation of bleb formation, the blebs typically grew to a size of $5\text{--}10\ \mu\text{m}$ (Figure 2d–g) and budded off into the solution over time. It was observed that dBBr caused more pronounced and earlier onset of blebbing than mBBr. In contrast to mBBr, dBBr is a bidentate thiol-reactive hapten (two reactive groups) and inherently facilitates cross-linking with free thiols in the cytoskeleton. Previously, it has been shown that extended cytoskeleton cross-linking provokes more extensive bleb formation,¹⁷ which could be a reason for the substantial blebbing induced by dBBr. On the other hand, mBBr being a monodentate compound possesses one thiol-reactive group and is thus unable to cause cross-linking. Nevertheless, as mBBr also induces blebbing, the data show that mere oxidation of cellular thiol groups is enough to lead to substantial shedding of membrane blebs.¹⁸

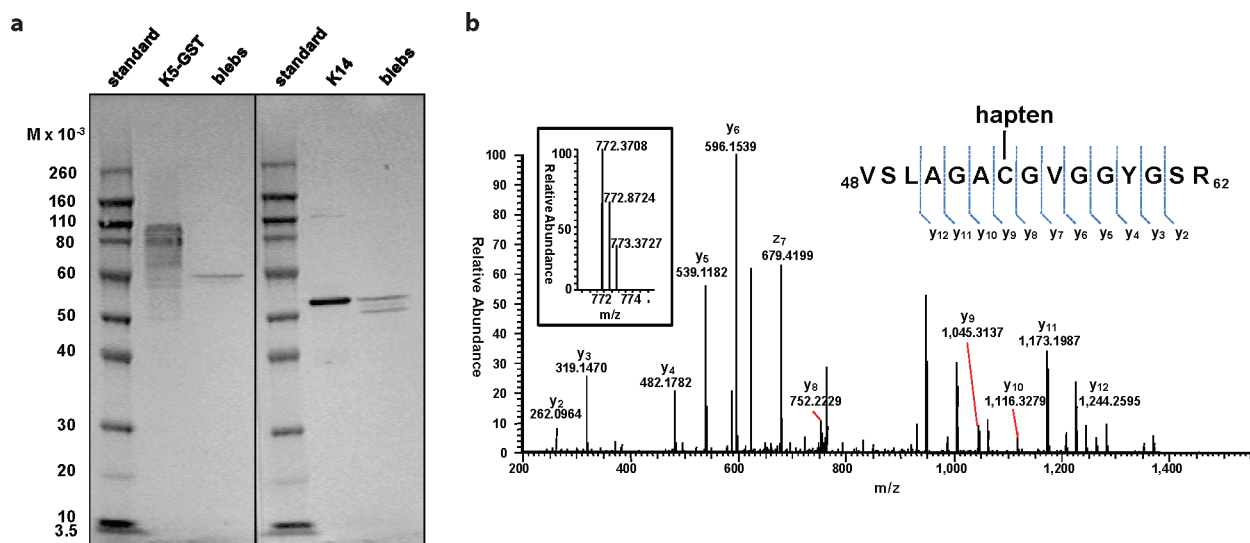


Figure 3. (a) Western blot of blebs extracted from keratinocytes exposed to the mBBR. Left panel: antikeratin 5 primary antibody. Right panel: antikeratin 14 primary antibody. All numbers indicate $M_R \times 10^3$. The K5 positive control carries a GST tag, explaining the higher molecular weight. (b) MS/MS fragmentation spectra of the tryptic fragment V48-R62 of K5, modified by mBBR at residue C54. Inset shows the M^{2+} ion with a m/z of 772.37. z_7 is the corresponding z ion of y_7 . Complete annotation of peaks is presented in the Supporting Information (Figure S2).

Interestingly, membrane integrity was unperturbed, while cells were shedding blebs until rapid decrease of the intracellular fluorescence denoted breakdown of membrane integrity. Cell death as the final consequence of hapten exposure was detected after ~ 5 h of postexposure using trypan blue as an indicator (Figure 2h). Weakly stained filamentous structures could still be detected in cells after cytosol leakout, which most likely represent cytoskeletal fluorescent HPC remnants (not shown). Neither of these events was seen upon methylbimane exposure, and again, the methylbimane uptake efficiency was very low with unspecific intracellular distribution, even after comparatively long exposure times for up to 1 h before medium replacement.

In response to bromobimanes but not to methyl bimane, migration or other visible morphological changes of the keratinocytes could no longer be detected and cells maintained unchanged morphology even after breakdown of membrane integrity. Nevertheless, plasma membrane blebs were still released over an observation period of up to 24 h. These responses resemble necrotic cell death, where irreversible formation of micrometer-sized blebs occurs. However, the keratinocytes do not display the typical morphological changes during necrosis, such as swelling before blebbing onset, cell disintegration, and cytosol spillout.^{19,20} To investigate whether cells were apoptotic, bromobimane-incubated cells were tested 4 and 7.5 h postincubation using an Annexin V and propidium iodide (PI)-based apoptosis assay kit. This kit defines apoptotic cells as having externalized phosphatidylserine (PS) without concomitant PI staining of DNA, the latter indicating compromised membranes present in necrotic cells. Blebbing was widely present after 4 h, but cell membranes were still intact, and no PS externalization was detected (not shown). After 7 h, most cells had PI-labeled nuclei and thus compromised membranes; however, no apoptotic cells were found (Figure 2i), indicating that the cells undergo a form of modified necrosis after hapten exposure.

Keratinocyte Blebs Contain K5 and K14. The filamentous fluorescent staining patterns in living keratinocytes and the identification of the keratins K5 and K14 as hapten targets in

skin⁵ raised the question if these keratins could also be identified in keratinocyte blebs. This notion was supported by the fact that the keratinocyte blebs were fluorescent. For analysis, blebs were separated and collected from keratinocytes 24 h posthaptentation with mBBR. The blebs were lysed and subjected to Western blot analysis, where the application of polyclonal anti-K5 and anti-K14 antibodies confirmed that the blebs indeed contained both K5 and K14 (Figure 3a). The presence of K5 and K14 was verified via mass spectrometry, where the corresponding fluorescent protein band in the SDS gel (not shown) was excised, subjected to tryptic digest, and analyzed via LC-MS/MS. Interestingly, the expected tryptic fragment from K5 was not recovered from mBBR-exposed keratinocytes (Supporting Information, Figure S1). However, manual investigation of the MS spectra revealed a peptide with an m/z of 772.37, a peptide fragment corresponding to the amino acids V48-R62 modified by one mBBR, which allowed pinpointing the exact site of haptentation on K5. Indeed, the MS2 spectra of the peptide uncovered the same tryptic V48-R62 peptide modified at cysteine 54 (C54) by mBBR (Figure 3b). These findings support our earlier results from excised skin tissue, where the unexpected K5 peptide fragment V48-R62 was found to be modified by mBBR at C54.⁵ In succession to our previous findings in ex vivo skin tissue, this is now the first time an exact site of haptentation has been shown in living cells. Bleb formation occurred faster and to a greater extent with the bidentate hapten dBBR than the monodentate mBBR, possibly due to cross-linking. Unfortunately, no cross-linked adducts could be detected in the mass spectrometer because of too high mass to charge ratios.

Intriguingly, the tryptic fragment containing cysteine C473 residing in the K5 tail region was found to be unmodified in the MS analysis (Supporting Information, Figure S1), implying that this residue does not react with the thiol-reactive hapten. This suggests that the tail region of K5 is more hidden and hence less available for modification as compared to the head region. Mass analysis also supported the findings that keratinocytes do not undergo apoptosis during blebbing. In vivo, keratinocytes are cleared by apoptosis via the formation of small vesicles, known as

keratin bodies (civatte bodies),^{21–23} containing caspase-cleaved K14 and hyperphosphorylated keratins as major constituents. However, in our findings, keratinocyte blebs contained only the intact keratins K5 and K14 (Figure 3a), and no hyperphosphorylation of the bleb-keratins could be detected in the mass analysis (Supporting Information, Figure S1), supporting the earlier statement that necrosis rather than apoptosis is induced in keratinocytes after bromobimane exposure.

DISCUSSION

The key steps of the sensitization phase of ACD, that is, which cells and proteins are primarily targeted, have until recently been obscure. In the present study, we strived to extend our previous investigation on hapten–target proteins in excised skin tissue⁵ to further explore the biological response to haptens in a living system. For this, the localization and biological consequences of exposing living keratinocytes to thiol-reactive fluorescent model haptens in vitro were investigated. On the basis of the fact that in hapten-exposed skin tissue, only keratinocytes in the basal layer were found to be hapten-labeled,⁵ we here studied the in vitro response of undifferentiated keratinocytes to the bromobimanes.

Consistent with the finding in skin tissue, the keratins K5 and K14 were found to be haptenated in living keratinocytes, where C54 was demonstrated to be a specific target. In addition, confocal microscopy revealed a localization pattern of the bromobimanes with similarities to the KIF network structure. As keratins make up $\geq 80\%$ of the total cellular protein in fully differentiated keratinocytes and up to 35% of the basal keratinocytes, it is not surprising that this protein represents a large target area for haptens. Furthermore, it should be noted that the K5 peptide is located at a linkage point between KIFs and desmosomes, which represents a crucial element for maintenance of epidermis cohesion.²⁴ No bimane-induced alterations in cell–cell interactions could be detected, which could be explained by the fact that in culture conditions, desmosome formation is suppressed in the first place.²⁵ However, as our observations are based solely on imaging of cell morphology, more elaborate methods would need to be employed to assess the effect of bimanens on intercellular adhesion in vitro.

Nevertheless, the observed hapten binding at C54 of K5, corresponding to the desmosome linkage point, leads us to speculate whether intercellular adhesion could be affected or lost in consequence of hapten exposure in vivo, leading to cell death. We observe that as a direct consequence of hapten exposure, cultured keratinocytes do indeed die along with the release of membrane blebs. Release of membrane vesicles is known during apoptosis and necrosis, where for example in skin, keratin bodies^{21–23} are released during apoptotic clearance in vivo. On the basis of our in vitro observations, it would thus be interesting to investigate whether hapten exposure induces keratinocyte mortality in vivo.

Analysis of the bleb content using mass spectrometry revealed that the keratinocyte blebs contained the same haptenated keratins as found in excised human skin.⁵ This result, in combination with the increasing focus on the role of membrane vesicles as active intercellular messengers,²⁶ spurs the interesting thought that the blebs might act as transport vesicles. So far, we have no data showing that keratinocyte blebs are formed in vivo, but there is evidence that keratin-antigens are formed in vivo, as anti-K14 antibodies have been detected in mouse serum after topical bromobimane exposure.⁵

Taking these results together, one could speculate that keratinocytes in vivo react similarly to hapten exposure, that is, expelling hapten-modified proteins in shedded membrane vesicles to the surroundings. The vesicles would then subsequently be taken up by skin resident DCs and hapten-modified keratin peptides presented as neoepitopes to T cells in the draining lymph nodes, triggering the acquired immune response (Supporting Information, Figure S3). Our proposed hypothesis needs to be further investigated to reveal if HPC complexes are excreted in this way in vivo. Also, it remains to be examined if keratin-containing HPCs are found in antigen-presenting cells, in vitro as well as in vivo, and if the correlation of keratinocyte blebbing with hapten exposure is a general phenomenon. Studies on the latter subject are currently underway.

ASSOCIATED CONTENT

S Supporting Information. Experimental protocols of two-photon fluorescence imaging of skin tissue and proteomic methods; figures describing K5 sequence coverage, complete annotation of peaks in MS2 spectra, and suggested ACD sensitization pathway; and supporting videos of bimane uptake over time. This material is available free of charge via the Internet at <http://pubs.acs.org>.

AUTHOR INFORMATION

Corresponding Author

*Tel: +46 31 786 9151. E-mail: brigitte.bauer@physics.gu.se.

Funding Sources

Financial support was obtained from Göteborg Science Centre for Molecular Skin Research at the University of Gothenburg and the Swedish Research Council.

Notes

B.B., S.I.A., A.-L.S., C.S., C.A.J., M.B.E., and K.B. have patents pending.

ACKNOWLEDGMENT

We thank the Proteomics Core Facility at Sahlgrenska Academy, University of Gothenburg, funded by a grant from the Knut and Alice Wallenberg Foundation. We thank Ann-Therese Karlberg, Department of Dermatochemistry, University of Gothenburg, for valuable input and for access to cell culturing facility and Owe Orwar, Physical Chemistry, Chalmers University of Technology, for access to the confocal microscope. K.B. also thanks Klas Broo for fruitful discussions.

ABBREVIATIONS

ACD, allergic contact dermatitis; dBB, dibromobimane; C54, cysteine 54; HPC, hapten–protein complex; K5, keratin 5; K14, keratin 14; LLNA, local lymph node assay; mBB, monobromobimane; GSH, glutathione; KIF, keratin intermediate filaments.

REFERENCES

- (1) Karlberg, A. T., Bergstrom, M. A., Borje, A., Luthman, K., and Nilsson, J. L. G. (2008) Allergic contact dermatitis-formation, structural requirements, and reactivity of skin sensitizers. *Chem. Res. Toxicol.* 21, 53–69.
- (2) Groot, A.; Frosch, P. (2006) Patch Test Concentrations and Vehicles for Testing Contact Allergens. *Contact Dermatitis*; Springer: Berlin; pp 907–928.
- (3) Thyssen, J. P., Linneberg, A., Menne, T., and Johansen, J. D. (2007) The epidemiology of contact allergy in the general population—Prevalence and main findings. *Contact Dermatitis* 57, 287–299.

- (4) Landsteiner, K., and Jacobs, J. (1935) Studies on the Sensitization of Animals with Simple Chemical Compounds. *J. Exp. Med.* 61, 643–656.
- (5) Simonsson, C., Andersson, S. I., Stenfeldt, A. L., Bergstrom, J., Bauer, B., Jonsson, C. A., Ericson, M. B., and Broo, K. S. (2011) Caged Fluorescent Haptens Reveal the Generation of Cryptic Epitopes in Allergic Contact Dermatitis. *J. Invest. Dermatol.* [Online early access] doi:10.1038/jid.2010.422. Published online: Jan 13, 2011. <http://www.nature.com/jid/journal/vaop/ncurrent/full/jid2010422a.html> [accessed Jan 13, 2011].
- (6) Basketter, D. A., Gerberick, F., and Kimber, I. (2007) The local lymph node assay and the assessment of relative potency: Status of validation. *Contact Dermatitis* 57, 70–75.
- (7) Aleksic, M., Pease, C. K., Basketter, D. A., Panico, M., Morris, H. R., and Dell, A. (2008) Mass spectrometric identification of covalent adducts of the skin allergen 2,4-dinitro-1-chlorobenzene and model skin proteins. *Toxicol. in Vitro* 22, 1169–1176.
- (8) Dietz, L., Esser, P. R., Schmucker, S. S., Goette, I., Richter, A., Schnolzer, M., Martin, S. F., and Thierse, H. J. (2010) Tracking human contact allergens: from mass spectrometric identification of peptide-bound reactive small chemicals to chemical-specific naive human T-cell priming. *Toxicol. Sci.* 117, 336–347.
- (9) Heiss, K., Junkes, C., Guerreiro, N., Swamy, M., Camacho-Carvajal, M. M., Schamel, W. W. A., Haidl, I. D., Wild, D., Weltzien, H. U., and Thierse, H. J. (2005) Subproteomic analysis of metal-interacting proteins in human B cells. *Proteomics* 5, 3614–3622.
- (10) Jenkinson, C., Jenkins, R. E., Aleksic, M., Pirmohamed, M., Naisbitt, D. J., and Park, B. K. (2010) Characterization of p-phenylenediamine-albumin binding sites and T-cell responses to hapten-modified protein. *J. Invest. Dermatol.* 130, 732–742.
- (11) Thierse, H. J., Moulon, C., Allespach, Y., Zimmermann, B., Doetze, A., Kuppig, S., Wild, D., Herberg, F., and Weltzien, H. U. (2004) Metal-protein complex-mediated transport and delivery of Ni²⁺ to TCR/MHC contact sites in nickel-specific human T cell activation. *J. Immunol.* 172, 1926–1934.
- (12) Meschkat, E., Barratt, M. D., and Lepoittevin, J. P. (2001) Studies of the chemical selectivity of hapten, reactivity, and skin sensitization potency. 2. NMR studies of the covalent binding of the C-13-labeled skin sensitizers 2-[C-13]- and 3-[C-13]hex-1-ene- and 3-[C-13]hexane-1,3-sultones to human serum albumin. *Chem. Res. Toxicol.* 14, 118–126.
- (13) Barker, J. N. W. N. (1992) Role of Keratinocytes in Allergic Contact-Dermatitis. *Contact Dermatitis* 26, 145–148.
- (14) Vocanson, M., Hennino, A., Rozieres, A., Poyet, G., and Nicolas, J. F. (2009) Effector and regulatory mechanisms in allergic contact dermatitis. *Allergy* 64, 1699–1714.
- (15) Gaspari, A. A., Jenkins, M. K., and Katz, S. I. (1988) Class-II Mhc-Bearing Keratinocytes Induce Antigen-Specific Unresponsiveness in Hapten-Specific Th1 Clones. *J. Immunol.* 141, 2216–2220.
- (16) Eklund, B. I., Edalat, M., Stenberg, G., and Mannervik, B. (2002) Screening for recombinant glutathione transferases active with monochlorobimane. *Anal. Biochem.* 309, 102–108.
- (17) Hagmann, J., Burger, M. M., and Dagan, D. (1999) Regulation of plasma membrane blebbing by the cytoskeleton. *J. Cell. Biochem.* 73, 488–499.
- (18) Scott, R. E., Perkins, R. G., Zschunke, M. A., Hoerl, B. J., and Maercklein, P. B. (1979) Plasma-Membrane Vesiculation in 3T3-Cells and Sv3T3-Cells 0.1. Morphological and Biochemical Characterization. *J. Cell Sci.* 35, 229–243.
- (19) Rello, S., Stockert, J. C., Moreno, V., Gamez, A., Pacheco, M., Juarranz, A., Canete, M., and Villanueva, A. (2005) Morphological criteria to distinguish cell death induced by apoptotic and necrotic treatments. *Apoptosis* 10, 201–208.
- (20) Ziegler, U., and Groscurth, P. (2004) Morphological features of cell death. *News Physiol. Sci.* 19, 124–128.
- (21) Ebner, H., and Gebhart, W. (1975) Light and Electron-Microscopic Differentiation of Amyloid and Colloid or Hyaline Bodies. *Br. J. Dermatol.* 92, 637–645.
- (22) Grubauer, G., Romani, N., Kofler, H., Stanzl, U., Fritsch, P., and Hintner, H. (1986) Apoptotic Keratin Bodies as Autoantigen Causing the Production of Igm-Anti-Keratin Intermediate Filament Autoantibodies. *J. Invest. Dermatol.* 87, 466–471.
- (23) Hosokawa, M., Masu, S. I., and Seiji, M. (1981) Immunofluorescence Studies on Civatte Bodies and Dyskeratotic Cells with Anti-Keratin Antibody. *Tohoku J. Exp. Med.* 135, 219–229.
- (24) Kouklis, P. D., Hutton, E., and Fuchs, E. (1994) Making a Connection—Direct Binding between Keratin Intermediate Filaments and Desmosomal Proteins. *J. Cell Biol.* 127, 1049–1060.
- (25) Inohara, S., Tatsumi, Y., Cho, H., Tanaka, Y., and Sagami, S. (1990) Actin Filament and Desmosome Formation in Cultured Human Keratinocytes. *Arch. Dermatol. Res.* 282, 210–212.
- (26) Thery, C., Ostrowski, M., and Segura, E. (2009) Membrane vesicles as conveyors of immune responses. *Nat. Rev. Immunol.* 9, 581–593.